ChemComm

Accepted Manuscript

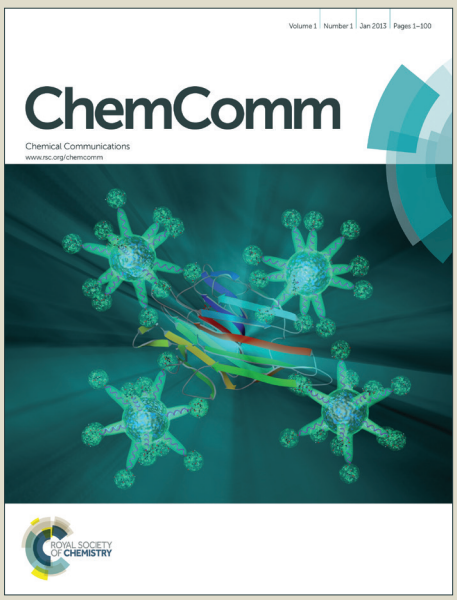

ROYAL SOCIETY OF CHEMISTRY

www.rsc.org/chemcomm

Cite this: DOI: 10.1039/c0xx00000x

www.rsc.org/xxxxxx

ARTICLE TYPE

Plasmon Resonance Tuning Using DNA Origami Actuation

Luca Piantanida[a], Denys Naumenko[a,b], Emanuela Torelli[c], Monica Marini[c[+],], Dennis M. Bauer[d], Ljiljana Fruk[d], Giuseppe Firrao[c], and Marco Lazzarino[a]

Received (in XXX, XXX) Xth XXXXXXXXX 20XX, Accepted Xth XXXXXXXXX 20XX

DOI: 10.1039/b000000x

A strategy for an innovative, continuous and reversible LSPR tuning using a DNA origami actuation to modulate the nanometric separation of two gold nanoparticles has been developed. The actuation mechanism is based on DNA hybridization, in particular three different DNA sequences were shown to induce resonance shift up to 6 nm.

Plasmons are collective oscillations of conduction band electrons at noble metal surfaces induced by the interaction with electromagnetic radiation, they dominate the optical properties in the visible range and have been extensively exploited for light manipulation and sensing.[1, 2] One of the most relevant application of plasmons exploits the field enhancement produced at surface edges and gaps to increase the Raman signal up to 10 orders of magnitude; this phenomenon is known as surface enhanced Raman scattering (SERS).[3]

In case of nanoparticles (NPs), plasmons are confined to the surfaces, are non-propagating and are known as localized surface plasmon resonance (LSPR).[4] The LSPR of isolated metal nanoparticles depends on the material, size, shape and permittivity of the medium in which they are embedded. This, in turn, leads to an intrinsic ability of tuning the resonance wavelength simply by changing one or more of these parameters.[5] In addition, the plasmon resonance of interacting nanoparticles also depends on the distance between them; the closer are the NPs, the longer is the resonance wavelength.[6] This effect has been used to build a plasmon ruler, which uses the resonance shift to precisely measure the distance of two known AuNP and hence the size of the objects to which the AuNP are linked.[7, 8] In such way, gold discs or triangles particles with controlled gaps have been fabricated by electron beam lithography to explore the effect of distance and shape on plasmonic resonance.[9] Different biomolecules, such as DNA of different lengths, were also used as spacers to tune the plasmon resonance of AuNPs.[10] An extremely fine tuning has been obtained by changing the geometrical parameters, the composition of NPs and the interparticle gap, however, in the vast majority of the reported examples this was achieved on separated structures therefore limiting the level of the control.[11] Only few examples of LSPR tuning were reported by changing the conformation of the same structure, using i.e a temperature or a pH modulation.[12] Zharnikov's group reported a reversible LSPR tuning dependent on the temperature of a polymer film within which gold NPs

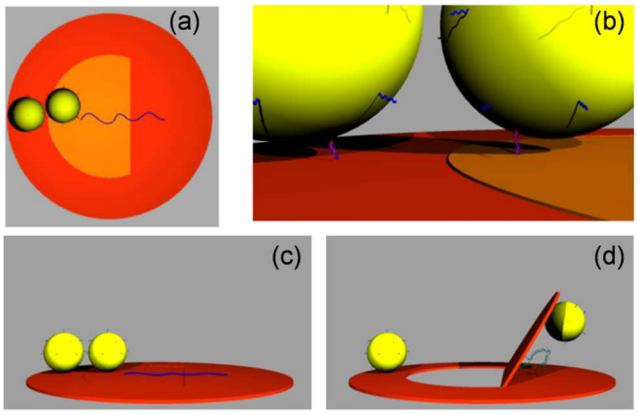

Fig. 1 Schematic representations of the DNA origami circular shape and linked gold nanoparticles hybrid structure. (a) Top view of the disc shape with the nanoparticles position according to the design, the ssDNA probe is schematized in blue and the flap portion is highlighted in orange. (b) Zoomed view of the linking zone between the two DNA coated NPs and the DNA origami: one on the external ring and the other (right) on the flap region. (c) The non actuated hybrid structure presents a close nanoparticles pair. (d) Example of hatch opening angle after the hybridization with the target.

(AuNP) were embedded.[13] Smith and co-workers exploited the NPs displacement on a spring-like molecular film, driven by polarity oscillation of an electrical field.[14] These studies tuned the plasmon resonance in finite steps between distinct fixed positions, obtaining a sort of digital modulations that are driven by discrete parameters. Au colloid nanospheres functionalized with DNA have been widely employed as a functional element in self assembled nano-architecture, because of the stability of Au in aqueous environment, and the simplicity of surface modification.[15] Due to its versatility and addressability by hybridization of complementary DNA strands, the DNA origami technology has opened new routes to building nano-objects such as a large variety of 2D/3D DNA constructs that could be engineered as a simple addressable platform for different molecules or metallic nanoparticles.[16-18] This technique provided additional advancement in design of self-assembled nanostructures[19-22] with particular focus on the plasmonic DNA-nanoparticles hybrid structures.[23-25]

Cite this: DOI: 10.1039/c0xx00000x

www.rsc.org/xxxxxx

ARTICLE TYPE

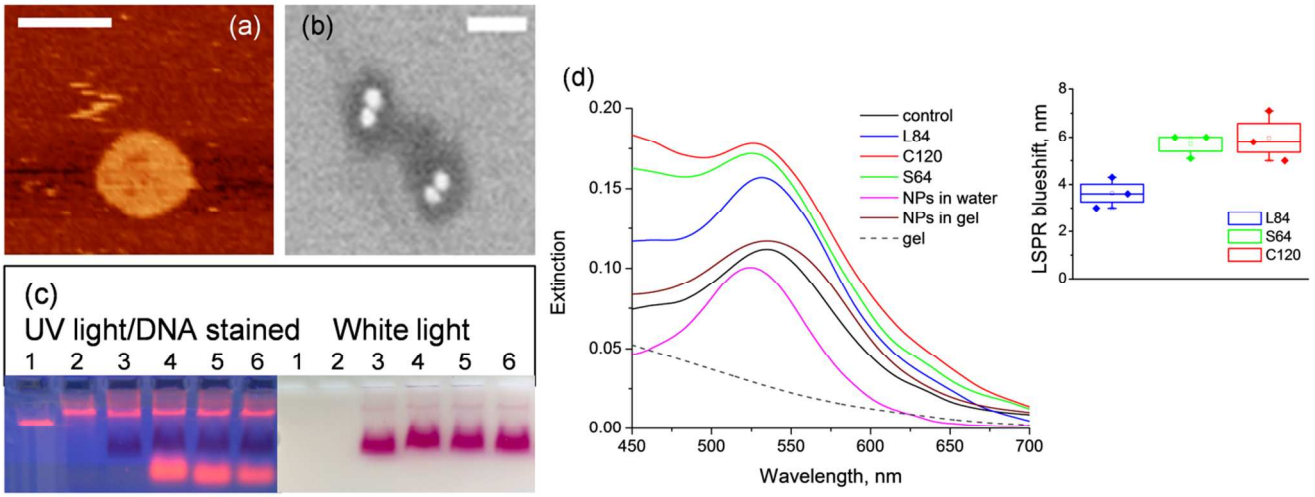

Fig. 2 (a) High resolution AFM images of a DNA origami before AuNP decoration (scale bar: 100 nm). (b) High resolution SEM image of a DNA origami after AuNP decoration (scale bar: 100 nm). The DNA origami 100 nm circle appears darker than the substrate because of electron beam induced charging. The AuNP appears brighter for their larger electron scattering cross section. (c) UV fluorescence (left section) and white light (right section) images of electrophoretic migration of DNA with and without AuNP. Lane 1: M13mp18 (scaffold) DNA control. Lane 2: DNA origami with no AuNP functionalization. Lane 3-6: DNA origami functionalized with nanoparticles and hybridized to: no target (control, lane 3), target C120 (lane 4), target L84 (lane 5) and target S64 (lane 6). A light red-colored band in white light picture indicates the linking between nanoparticles and DNA origami (see also Fig. S3, ESI†). (d) Raw UV-Vis extinction spectra from the origami bands described in panel (c): a blue shift is visible for all the targets in respect to the control. In the inset the box plots of the three targets relative shifts repeated three times are reported. The LSPR positions were determined after fitting procedure described in ESI†, Fig. S8.

In this study we report on the continuous analog tuning of the LSPR in AuNP dimer obtained using a DNA origami scaffold. We designed a DNA origami made of an external disc (100 nm diameter) with a movable internal hatch. The hatch hinges are made by single strand insertions along the conjugation line (Fig. 1a and S1, ESI†). A 120 nucleotides (nts) long single strand DNA (ssDNA) probe connects the hatch tip to the external fixed disc. Upon hybridization with a proper target, a coiled dsDNA strand is formed with a shorter length. As a result the hatch is lifted out of plane, with an angle that depends on the probe sequence and on the degree of hybridization.

A similar strategy was already adopted in our previous work and, upon the proper choice of target and probe sequences, was demonstrated to be reversible.[26]

In order to decorate the DNA origami hatch structure, 20 nm gold colloids (Ted Pella Inc.) were functionalized with thiol-capped DNA oligonucleotides following a published procedure.[27] To arrange one NP on the external ring and one on the edge of the internal flap (Fig. 1a-b). Two scaffold-sequence portions were left free to hybridize with the NP linked oligonucleotides.

In this way two 20 nm AuNP were placed in contact with each other when the hatch is closed as shown in Fig. 1a-b-c. As in the previous report, the target-probe hybridization reduces the end-to-end distance of about 35% thus generating an actuation tension that opens the hatch.[26] The opening width – or angle – depends on the specific hybridization path and on the target sequence. However, the balance between the hybridization forces and dsDNA mechanics is still an open issue and a set of general rules to be used for optimization is still missing.[28, 29] Using this closing/opening principle, the precise tuning of the optical properties of DNA-plasmonic constructs could be obtained. In order to produce different opening angles we tested two fully complementary targets: a linear sequence 84 nts long (L84), and an hairpin sequence 120 nts long which includes in the central part the same sequence of the L84 target (C120); and a partially complementary linear target 64 nts long (S64) (Table S1, ESI†).

The DNA origami formation was verified by atomic force microscopy (AFM) in Mg^{2+} buffer, revealing a compact circular shape corresponding to the initial design (Fig. 2a and Fig. S4, ESI†).

The presence of hybridized AuNPs on the DNA origami was confirmed by gel electrophoresis. Both visible (for AuNP) and UV (for DNA stained with GelRed™) images of the same gel were taken and the band positions were compared. In this way we were able to uniquely associate a band corresponding to AuNP decorated DNA-origami (Fig. S3, ESI†). The origami extracted from this band were characterized by scanning electron microscopy (SEM) confirming the presence of two AuNPs (Fig. 2b and Fig. S6, ESI†).

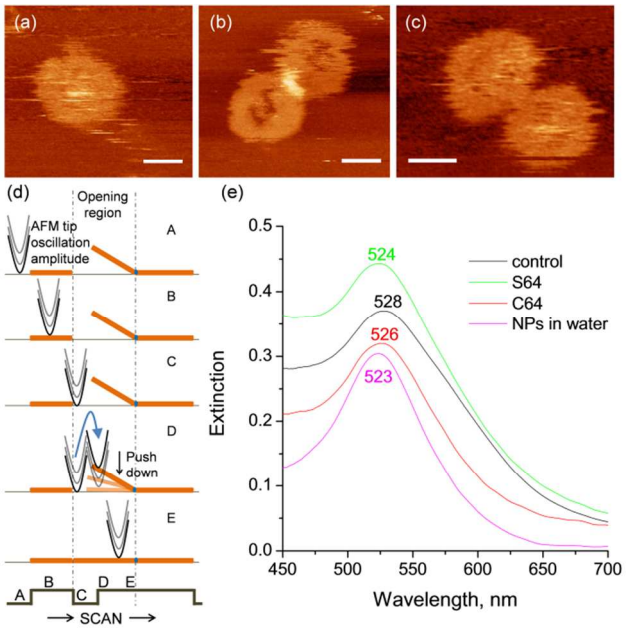

Fig. 3 AFM zoomed images of the DNA origami structures without gold NPs showing the reversibility of the hatch system using S64 target (scale bars: 50 nm). The origami is closed subsequently to (a) no target addition, (b) open after S64 addition and (c) re-closed after C64 addition. (d) Schematics of AFM-tip/origami interaction in non-contact mode: as the tip jumps on top of the open hatch, it pushes it down so, only a tiny line is observable in the open configuration. (e) Background subtracted UV-Vis extinction spectra of gold NPs decorated origami in gel that report representative measurement of the reversibility tuning of LSPR with the hatch origami system: target S64 presents blue shift in respect to the control (no target addition) suggesting the opening of the flap. After the addition of the competitor C64 this blue shift is decreased suggesting a partial re-closure of the system. The AuNPs in water show the control situation in which no LSPR coupling is present between them.

In order to demonstrate the effective tuning of the interparticles distance and thus of the plasmon resonance, we incubated the AuNP-origami structures with each one of the three DNA targets required for the hatch opening. The results of the agarose gel electorphoresis of the three hybridized samples is shown in Fig. 2c. The UV image relative to DNA staining is aligned to the white light image where the contrast is provided by the AuNP plasmonic absorption. The first and second wells were filled with the scaffold sequence (M13mp18) and the DNA origami respectively, which show a signal only in the UV section, since there are no AuNP to provide a contrast in the visible absorbance region. The correctly folded DNA origami migrates slower than the linear scaffold (Fig. 2c, lane 2) and it is used as reference for the other lanes. The DNA origami incubated with NPs is included in all of the remaining lanes (Fig. 2c, lanes 3-6), which differ only in target sequence. In detail, the lane 3 is used as a control and no DNA target is added, while the targets C120, L84 and S64 are added to lanes 4, 5 and 6, respectively. The targets are usually mixed in excess (2 µL of 8 µM), to induce complete hybridization to DNA origami, and the unbound DNA oligonucleotides, which migrate faster in gel, form broad downstream bands visible only in the UV images. In the case of C120 target, the excess DNA moves slightly slower within gel due to the longer sequence (Fig. 2c, lane 4). The match between the DNA origami band and a light red-colored band obtained under white light indicates the linking between NPs and DNA origami. The excess of unbound NPs can be observed as the broad red band in all the lanes and is negative upon DNA staining. No difference in the bands position is observed between the control and the three DNA target-actuated constructs. The structural differences induced by the target hybridization are not large enough to produce an appreciable electrophoretic migration delay. A few weak, slowly moving bands can be observed that are attributed to the formation of DNA origami superstructures (dimers, tetramers, etc.) as it was also confirmed by AFM and SEM (Fig. S4 and S5, ESI†).

The extinction spectra for each structure were recorded directly on the separated gel bands to minimize cross band contamination, gel extraction induced damage, and complex re-concentration procedures. The raw spectra are displayed in figure 2d together with the extinction spectra of DNA coated gold NPs in gel and water. Note that NPs in gel form highly packed aggregates and this, together with higher dielectric permittivity of gel, results in significant red shift of LSPR peak and its broadening due to a plasmon coupling effect in respect to origami with gold NPs.[4] All the three targets induced a blue shift and a narrowing of the spectra with respect to the control, however the spectra differ significantly in the background contribution, which we attributed to gel thickness variability. The experiments were replicated 3 times with different origami synthesis. We consistently observed an LSPR blue shift although absolute values were slightly different. To discard the background contribution and compare the results of different experiments we applied the fitting procedure described in details in ESI† (Fig. S8). The C120 and S64 target sequences produce a relative blue shift of ~6 nm, while the L84 target provided only ~4 nm (Fig. 2d inset). The relative shift depends only on the AuNP separation controlled by the addition of the three targets, since all the other contributions, namely gel density, gel hydration and AuNP size[4], are common to all experiments. The large shift provided by S64 and C120 is consistent with the competitors design, and in particular with the reduced length of the S64 sequence and the hairpin structure of the C120 in contrast with the full linear structure of the L84 target.[29] Since the probe sequences can be arbitrary varied, the plasmonic resonance can be tuned continuously from the fully closed to the fully opened configuration: three points along this range are exemplified here. The measurement of the plasmon resonance shift can be used to deduce the actual opening angle for each configuration; however a better modelling of the gel-AuNP optical response should be first developed, which is beyond the scope of this communication.

The reversibility of the LSPR tuning was investigated by AFM microscopy in absence of AuNP and by UV-Vis spectroscopy after decorating the origami with the AuNP. To this purpose, following a previous reported strategy[26], we exploited the partial complementarity of the S64 to the actuator. A "competitor" (C64, Table S1, ESI†) DNA strand fully complementary to the S64 was used to detach, by higher affinity, the target from actuator. In Fig. 3a-c AFM images of the origami in the closed, open and reclosed

position are displayed. The extinction spectra before and after adding the S64 target, and then after adding the C64 competitor are displayed in figure 3e. The target induces a blue shift of 4 nm; the addition of the competitor reduces - but do not cancel - the shift to 2 nm. This only partial flap re-closure with respect to situation observed by AFM imaging could be originated by a modification of the origami mechanical properties due to the AuNP-induced mass and surface increase.

Conclusions

In conclusion, we have exploited a DNA origami to tune the plasmon resonance between two gold nanospheres. The particular actuation mechanism design has allowed us to produce a continuous, or analog, tuning of the interparticles distance in aqueous solution. The resulting resonance blue shifts and narrowing of LSPR peaks were observed in three different configurations. The actuation mechanism, based on hybridization with ssDNA targets, opens a wide range of possibilities for the fine manipulation of angles and dynamics between nanostructured components, depending on the secondary structure of the DNA filament. The proposed design is suitable to investigate DNA hybridization configurations, or could be used as tunable plasmonic platform for enhanced Raman applications.

This work was partially founded by FET Project "Single Molecule Detection and Activation", CFN Project A.5.7 and TALENTS UP Programme (7th R&D Framework Programme: PEOPLE – Marie Curie Actions – COFUND). We aknowledge Loredana Casalis and Mattia Fanetti for providing access to the AFM and SEM microscopes.

Notes and references

[a] *CNR-IOM Laboratorio TASC, Area Science Park, Basovizza, 34149, Trieste, Italy. Email: piantanida@iom.cnr.it; Tel: +39 040 3756458*
[b] *AREA Science Park, Padriciano 99, 34149 Trieste, Italy.*
[c] *Dipartimento di Scienze Agrarie e Ambientali, Università di Udine, via delle Scienze 206, 33100 Udine, Italy.*
[d] *Karlsruhe Institute of Technology (KIT) DFG-Centre for Functional Nanostructures (CFN) Wolfgang Gaede Str. 176131 Karlsruhe, Germany.*
[+] *Present address: King Abdullah University of Science and Technology Physical Science & Engineering Division, Kingdom of Saudi Arabia.*

† Electronic Supplementary Information (ESI) available: [DNA origami design and preparation, DNA targets sequences, electrophoresis separation of AuNPs-DNA origami sample, more AFM and SEM imaging characterization and the direct gel measurement procedure]. See DOI: 10.1039/b000000x/

1 P. K. Jain, X. Huang, I. H. El-Sayed and M. A. El-Sayed, *Acc Chem Res*, 2008, **41**, 1578-1586.
2 P. Alivisatos, *Nat. Biotechnol.*, 2004, **22**, 47-52.
3 G. V. P. Kumar, *Journal of Nanophotonics*, 2012, **6**, 064503-064501-064503-064520.
4 N. J. Halas, S. Lal, W. S. Chang, S. Link and P. Nordlander, *Chem. Rev.*, 2011, **111**, 3913-3961.
5 A. Klinkova, R. M. Choueiri and E. Kumacheva, *Chem. Soc. Rev.*, 2014, **43**, 3976-3991.
6 P. Nordlander, C. Oubre, E. Prodan, K. Li and M. I. Stockman, *Nano Lett.*, 2004, **4**, 899-903.
7 G. L. Liu, Y. Yin, S. Kunchakarra, B. Mukherjee, D. Gerion, S. D. Jett, D. G. Bear, J. W. Gray, A. P. Alivisatos, L. P. Lee and F. F. Chen, *Nat. Nanotechnol.*, 2006, **1**, 47-52.
8 P. K. Jain, W. Huang and M. A. El-Sayed, *Nano Lett.*, 2007, **7**, 2080-2088.
9 C. Tabor, R. Murali, M. Mahmoud and M. A. El-Sayed, *J. Phys. Chem. A*, 2009, **113**, 1946-1953.
10 B. M. Reinhard, M. Siu, H. Agarwal, A. P. Alivisatos and J. Liphardt, *Nano Lett.*, 2005, **5**, 2246-2252.
11 S. J. Barrow, A. M. Funston, X. Wei and P. Mulvaney, *Nano Today*, 2013, **8**, 138-167.
12 X. Liu, X. Wang, L. Zha, D. Lin, J. Yang, J. Zhou and L. Zhang, *Journal of Materials Chemistry C*, 2014, **2**, 7326-7335.
13 N. Meyerbroker, T. Kriesche and M. Zharnikov, *ACS Appl Mater Interfaces*, 2013, **5**, 2641-2649.
14 J. J. Mock, R. T. Hill, Y. J. Tsai, A. Chilkoti and D. R. Smith, *Nano Lett*, 2012, **12**, 1757-1764.
15 D. Zanchet, C. M. Micheel, W. J. Parak, D. Gerion and A. P. Alivisatos, *Nano Lett.*, 2000, **1**, 32-35.
16 Y. C. Hung, D. M. Bauer, I. Ahmed and L. Fruk, *Methods*, 2014, **67**, 105-115.
17 B. Ding, Z. Deng, H. Yan, S. Cabrini, R. N. Zuckermann and J. Bokor, *J. Am. Chem. Soc.*, 2010, **132**, 3248-3249.
18 X. Shen, Q. Jiang, J. Wang, L. Dai, G. Zou, Z. G. Wang, W. Q. Chen, W. Jiang and B. Ding, *Chem Commun*, 2012, **48**, 11301-11303.
19 P. W. Rothemund, *Nature*, 2006, **440**, 297-302.
20 S. M. Douglas, H. Dietz, T. Liedl, B. Hogberg, F. Graf and W. M. Shih, *Nature*, 2009, **459**, 414-418.
21 B. Sacca and C. M. Niemeyer, *Chem. Soc. Rev.*, 2011, **40**, 5910-5921.
22 E. Torelli, M. Marini, S. Palmano, L. Piantanida, C. Polano, A. Scarpellini, M. Lazzarino and G. Firrao, *Small*, 2014, **10**, 2918-2926.
23 X. Shen, P. Zhan, A. Kuzyk, Q. Liu, A. Asenjo-Garcia, H. Zhang, F. J. de Abajo, A. Govorov, B. Ding and N. Liu, *Nanoscale*, 2014, **6**, 2077-2081.
24 X. Shen, C. Song, J. Wang, D. Shi, Z. Wang, N. Liu and B. Ding, *J. Am. Chem. Soc.*, 2012, **134**, 146-149.
25 X. Lan, Z. Chen, G. Dai, X. Lu, W. Ni and Q. Wang, *J. Am. Chem. Soc.*, 2013, **135**, 11441-11444.
26 M. Marini, L. Piantanida, R. Musetti, A. Bek, M. Dong, F. Besenbacher, M. Lazzarino and G. Firrao, *Nano Lett.*, 2011, **11**, 5449-5454.
27 L. Piantanida, D. Naumenko and M. Lazzarino, *RSC Advances*, 2014, **4**, 15281-15287.
28 M. Zoli, *Soft Matter*, 2014, **10**, 4304-4311.
29 R. Vafabakhsh and T. Ha, *Science*, 2012, **337**, 1097-1101.